

# Quasi steady-state simulation diagnosis using Newton method with optimal multiplier

Patricia Rousseaux

Thierry Van Cutsem, *Fellow, IEEE*

**Abstract**—This paper deals with the quasi steady-state approximation of the long-term dynamics. This fast time simulation method assumes that the short-term dynamics are stable and can be replaced by their equilibrium equations. When the latter stop having a solution, the simulation undergoes a singularity. This paper proposes a method to identify which component(s) are responsible for the loss of equilibrium. The corresponding equations are identified using the Newton method with optimal multiplier. The method has been validated with respect to full time simulation. Very good results are shown on the Nordic-32 system, in cases where long-term voltage instability triggers loss of synchronism. The proposed method enhances time simulation at very low computational cost and can also help correcting model and/or operating point errors.

**Index Terms**—Long-term dynamics, voltage stability, time-domain simulation, quasi steady-state approximation, singularity, Newton method, line search

## I. INTRODUCTION

In power system dynamic studies, the trend is to perform numerical simulations over longer periods of time, with more detailed models, and for more operating conditions and disturbances. However, power system dynamic models are large and involve very different time scales, which makes their simulation over long time intervals very demanding.

Time-scale simplification of the model is a natural response to this complexity. The idea is not new. For instance, it underlies the quasi-sinusoidal (or phasor) approximation used in most stability studies [1], where electromagnetic transients are neglected and the network is modeled by algebraic equations.

The idea is further exploited in the Quasi Steady-State (QSS) approximation of long-term dynamics, which consists of replacing the short-term differential equations of generators, motors, compensators, etc. by the corresponding algebraic equilibrium equations. QSS simulation is well suited to computationally intensive tasks such as security limit determination, real-time applications or training simulators [2], [3].

Replacing the short-term dynamics by their equilibrium equations requires that dynamics to be stable. Now, in some degraded situations, it may happen that these dynamics lose their equilibrium point. This may correspond for instance to synchronous generators going out of step (angle instability) or induction motors stalling.

P. Rousseaux (p.rousseaux@ulg.ac.be) is with the Dept. of Electrical Engineering and Computer Science (Montefiore Institute) of the University of Liège, Sart Tilman B37, B-4000 Liège, Belgium. T. Van Cutsem (t.vanputsem@ulg.ac.be) is with the Belgian National Fund for Scientific Research (FNRS) at the same department.

When this happens, the QSS model meets a singularity. In practice, the Newton iterations diverge, and the simulation cannot proceed.

If it results from a loss of equilibrium, the singularity is by itself an indication that the system is subject to short-term instability. Using the method described in this paper, the objective will be to further identify which system components are responsible for this instability.

On the other hand, the singularity might result from a numerical problem, i.e. a lack of convergence of the Newton iterations. In this case, the proposed method is expected to solve the QSS equations by performing more careful Newton iterations.

To this purpose a scaling factor is applied to the Newton corrections as soon as an increase of the sum of squared mismatches is detected. The scaling factor is adjusted to minimize that sum, using a line search in the direction of the Newton correction. By so doing, the mismatches tend to concentrate on the subset equations most responsible for the infeasibility.

To the authors' knowledge, this optimal multiplier technique has been mainly applied to standard load flow equations. It was initially proposed in [4] to deal with ill-conditioned load flow problems. The diagnosis capability of the method was exploited in [5] to rank contingencies according to their impact on voltages. In [6], [7] the method was used in unsolvable load flow cases related to voltage instability, first as a solvability measure, then to identify minimal corrective actions to restore feasibility. Further in-depth analytical investigations were reported in [8].

This paper, on the contrary, deals with short-term equilibrium equations, allowing to validate the output of the method with respect to detailed time simulation.

## II. QSS APPROXIMATION: PRINCIPLE AND SINGULARITIES

### A. Principle of the QSS approximation

In stability studies, the general model of a power system takes on the Differential-Algebraic (DA) form:

$$\mathbf{0} = \mathbf{g}(\mathbf{x}, \mathbf{y}, \mathbf{z}) \quad (1)$$

$$\dot{\mathbf{x}} = \mathbf{f}(\mathbf{x}, \mathbf{y}, \mathbf{z}) \quad (2)$$

$$\mathbf{z}(t_k^+) = \mathbf{h}(\mathbf{x}, \mathbf{y}, \mathbf{z}(t_k^-)) \quad (3)$$

For an  $N$ -bus system, the  $2N$  algebraic equations (1) relate to the network and involve the vector  $\mathbf{y}$  of bus voltages.

The differential equations (2), involving the vector  $\mathbf{x}$  of continuous states, relate to a wide variety of phenomena and controls including:

- the short-term dynamics of generators, turbines, governors, Automatic Voltage Regulators (AVRs), Static Var Compensators, induction motors, HVDC links, etc.
- the long-term dynamics of secondary frequency and voltage control, load self-restoration, etc.

The discrete-time equations (3) capture discrete events that stem from:

- controllers acting on shunt compensation, generator set-points, Load Tap Changers (LTCs), etc. [1], [9]
- equipment protections such as OverExcitation Limiters (OELs), etc. [1], [9]
- system protection schemes acting on loads and/or generators.

The corresponding (shunt susceptance, transformer ratio, etc.) variables are grouped into  $\mathbf{z}$ , which undergoes step changes from  $\mathbf{z}(t_k^-)$  to  $\mathbf{z}(t_k^+)$  at some times  $t_k$ , most often dictated by the whole system dynamics.

As indicated previously, the QSS approximation of long-term dynamics consists of representing faster phenomena by their equilibrium conditions instead of their full dynamics. The correspondingly simplified model takes on the form:

$$\mathbf{0} = \mathbf{g}(\mathbf{x}_1, \mathbf{x}_2, \mathbf{y}, \mathbf{z}) \quad (4)$$

$$\mathbf{0} = \mathbf{f}_1(\mathbf{x}_1, \mathbf{x}_2, \mathbf{y}, \mathbf{z}) \quad (5)$$

$$\dot{\mathbf{x}}_2 = \mathbf{f}_2(\mathbf{x}_1, \mathbf{x}_2, \mathbf{y}, \mathbf{z}) \quad (6)$$

$$\mathbf{z}(t_k^+) = \mathbf{h}(\mathbf{x}_1, \mathbf{x}_2, \mathbf{y}, \mathbf{z}(t_k^-)) \quad (7)$$

in which  $\mathbf{x}$  (resp.  $\mathbf{f}$ ) has been decomposed into  $\mathbf{x}_1$  and  $\mathbf{x}_2$  (resp.  $\mathbf{f}_1$  and  $\mathbf{f}_2$ ).

Three algebraic equations (5) can be used to describe each generator, accounting for saturation, AVR voltage droop and governor speed droop effects [2], [3]. These equations are detailed in Appendix A.

System frequency is a component of  $\mathbf{x}_1$ , if its dynamics are neglected. This additional variable is balanced by the equation setting the voltage phase angle to zero at a reference bus [2].

In principle, (6) relates to long-term dynamics, and hence  $\mathbf{x}_2$  are the “slow” state variables. However, if frequency dynamics are taken into account, it may be required for accuracy purposes to retain some time constants in the order of a second in the (hydro) turbine and speed governor models, as reported in [10]. The corresponding differential equations are included in (6). Assuming the same speed for all generators and accounting for their inertia, the rate of change of frequency provides an additional equation (6). Frequency is then a component of  $\mathbf{x}_2$ .

### B. Singularities of the QSS approximation

While the assumption that the short-term dynamics are stable holds in most practical long-term stability studies [3], [2], [10], [11], it is invalidated in the following situations:

- 1) following a large disturbance, the system has a short-term equilibrium point but is not attracted by the latter. This is typical of transient (angle) instability, which takes place over a few seconds after the disturbance;
- 2) as  $\mathbf{x}_2$  and  $\mathbf{z}$  evolve according to the long-term dynamics, the short-term equilibrium becomes oscillatory unstable;

- 3) as  $\mathbf{x}_2$  and  $\mathbf{z}$  evolve according to the long-term dynamics, the short-term equilibrium disappears.

The first two cases cannot be detected by the QSS simulation. Coupling with detailed time simulation has been proposed in [11] to deal with the first case. The second case would require additional eigenvalue analysis. This paper focuses on the third case.

When the short-term equilibrium point disappears, the QSS equations can no longer be solved; the QSS model meets a singularity. Note that as the latter is approached, the time decoupling assumption is less and less valid and the “short-term” dynamics stop being “faster” [12]. Hence, before reaching a singularity, the QSS model (4-7) is expected to somewhat depart from the reference model (1-3).

QSS singularities may be encountered:

- 1) following discrete transitions (7) such as LTC movements or OEL activations. In this case, equations (4,5) cannot be solved for the updated value  $\mathbf{z}(t_k^+)$  and the current (unchanged) value of  $\mathbf{x}_2$ ;
- 2) immediately after an external disturbance, for which no post-disturbance short-term equilibrium exists. This case is similar to the previous one (with other parameters than  $\mathbf{z}$  undergoing a discontinuity);
- 3) due to a change in the continuous states  $\mathbf{x}_2$ , making it impossible at some time  $t^*$  to proceed to time  $t^* + h$ , where  $h$  is the simulation time step. If a partitioned scheme is used to integrate the DA model (4-7), a value is assumed (iteratively) for  $\mathbf{x}_2(t^* + h)$  and the singularity occurs in the course of solving (4,5) for the so updated value of  $\mathbf{x}_2$  and the current (unchanged) value of  $\mathbf{z}$ . If a simultaneous scheme is used, the equations that cannot be solved include additional relationships stemming from the discretization of (6).

Without loss of generality, we assume that a partitioned scheme is used. Hence, the equations to be handled are (4,5). In a  $g$ -generator system, there are  $2N + 3g + 1$  such equations (one of them setting the phase angle at a reference bus). To keep the notation simple, they are rewritten in compact form as:

$$\boldsymbol{\varphi}(\mathbf{u}) = \mathbf{0} \quad \text{with } \boldsymbol{\varphi} = \begin{bmatrix} \mathbf{g} \\ \mathbf{f}_1 \end{bmatrix} \quad \text{and } \mathbf{u} = \begin{bmatrix} \mathbf{y} \\ \mathbf{x}_1 \end{bmatrix} \quad (8)$$

### III. NEWTON METHOD WITH OPTIMAL MULTIPLIER

According to the well-known Newton method, equation (8) is solved through the following iterations:

$$\mathbf{u}^{k+1} = \mathbf{u}^k + \Delta\mathbf{u}^k \quad k = 0, 1, 2, \dots \quad (9)$$

with the correction  $\Delta\mathbf{u}^k$  given by:

$$\Delta\mathbf{u}^k = -\boldsymbol{\varphi}_{\mathbf{u}}^{-1}(\mathbf{u}^k)\boldsymbol{\varphi}(\mathbf{u}^k) \quad (10)$$

where  $\boldsymbol{\varphi}_{\mathbf{u}}(\mathbf{u}^k)$  stands for the Jacobian matrix of  $\boldsymbol{\varphi}$  with respect to  $\mathbf{u}$  at the  $k$ -th iteration. The above iterations converge rapidly provided the initial guess  $\mathbf{u}^0$  is sufficiently close to the solution. In case of ill-conditioned systems, however, the procedure may fail to converge. On the other hand, in case of a singularity, the system (8) has no solution and the Newton iterations (9) diverge.

A more robust scheme is as follows. Let us denote by  $\rho$  the sum of squared equation mismatches:

$$\rho = \boldsymbol{\varphi}^T(\mathbf{u})\boldsymbol{\varphi}(\mathbf{u}) = \sum_i \varphi_i^2(\mathbf{u}). \quad (11)$$

Let us first recall that the Newton step (10) is a descent direction for the  $\rho$  function. Indeed, the gradient of  $\rho$  is given by:

$$\nabla \rho = 2 \boldsymbol{\varphi}_u^T \boldsymbol{\varphi}$$

and hence:

$$\nabla \rho^T \Delta \mathbf{u} = -2 \boldsymbol{\varphi}^T \boldsymbol{\varphi} = -2 \rho < 0. \quad (12)$$

When the equations have a solution and the standard Newton scheme converges satisfactorily, the  $\rho$  function decreases from one iteration to the next, and tends to zero. In difficult cases, however, this may no longer hold because the step taken along the descent direction is too large. Therefrom the idea of applying a scalar multiplier  $\lambda$  to the correction so that  $\rho$  decreases from one iteration to the next.

To this purpose,  $\rho$  is computed at each iteration and, as long as the “full” Newton step (10) reduces  $\rho$ , i.e.  $\rho(\mathbf{u}^{k+1}) < \rho(\mathbf{u}^k)$ , one proceeds with the iterations (9,10). On the other hand, if an increase in  $\rho$  is detected, iterations are restarted and the correction is scaled at each iteration according to:

$$\mathbf{u}^{k+1} = \mathbf{u}^k + \lambda \Delta \mathbf{u}^k \quad \text{with } 0 \leq \lambda \leq 1. \quad (13)$$

The objective is to move along the direction of the Newton correction  $\Delta \mathbf{u}^k$  up to reaching the point which minimizes  $\rho$ . Since the Newton step is a descent direction for  $\rho$ , it is guaranteed to find an optimal step and the corresponding optimal multiplier  $\lambda_{min}$  by backtracking along this direction.

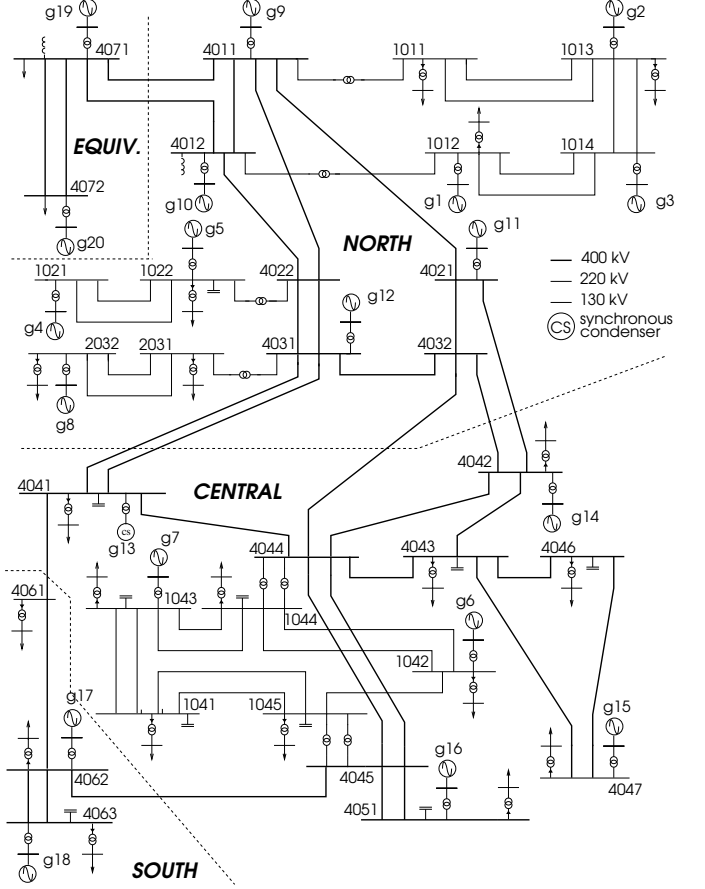
Thus, at each iteration, a line search is performed to solve the optimization problem:

$$\min_{\lambda \in [0, 1]} \rho(\mathbf{u}^k + \lambda \Delta \mathbf{u}^k).$$

To this purpose, we use a variant of the *golden search* method [13]. This technique does not require to evaluate the derivative of  $\rho$  with respect to  $\lambda$ . It simply relies on the assumption that  $\rho$  has no more than one minimum in the search interval. According to the authors’ experience, this is usually the case with the equations of the QSS model (as it is with load flow equations [8]). Note that since the objective is to “damp” the Newton iterations, no attempt is made to use  $\lambda_{min} > 1$ . More details are given in Appendix B.

The convergence of the overall procedure is achieved as soon as either: (i) all mismatches  $\varphi_i(\mathbf{u}^k)$  fall below a specified tolerance, or (ii)  $\lambda_{min}$  reaches a zero value. In both cases, divergence has been prevented since  $\rho(\mathbf{u}^{k+1})$  cannot be greater than  $\rho(\mathbf{u}^k)$ . Case (ii) corresponds to (8) having no solution. At the last reached point  $\mathbf{u}^*$ ,  $\rho$  has a nonzero value that cannot be further reduced and the mismatches  $\varphi_i(\mathbf{u}^*)$  tend to concentrate on the equations most responsible for the lack of solution. In other words, the final mismatches point out the system components most responsible for the singularity. The Jacobian matrix  $\boldsymbol{\varphi}_u$  is near singular [6], [7].

Within the context of QSS simulation, the optimal multiplier technique is expected to be triggered only when the singularity



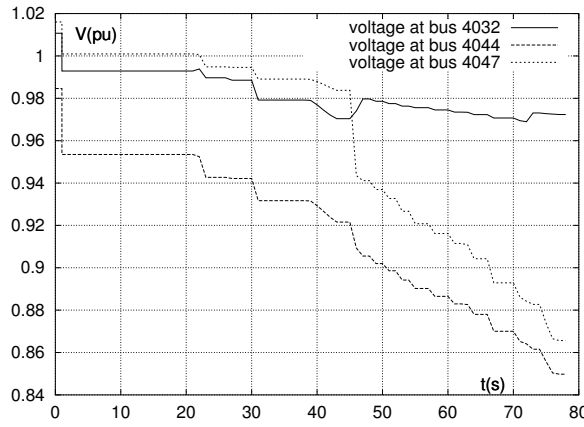


Fig. 2. Case 1. Time evolution of voltages - QSS simulation

### B. Case 1

We simulate the tripping, at  $t = 1$  s, of the 400-kV transmission line between buses 4032 and 4044.

The long-term evolution of voltages provided by QSS simulation is shown in Fig. 2. The system evolves under the effect of LTCs and OELs. For already mentioned reasons, many machines have their field currents limited: g7 at  $t = 22$ , g14 at  $t = 23$ , g12 at  $t = 27$ , g15 at  $t = 46$ , g16 at  $t = 47$ , and g6 at  $t = 73$  s.

The QSS simulation meets a singularity at  $t = 79$  s. At this time step, following the operation of four LTCs, Eqs. (4,5) can no longer be solved.

The results of the optimal multiplier method in terms of final mismatches are shown in Table I. The tolerances used to stop the Newton iterations are 0.5 MW (resp. Mvar) for active (resp. reactive) power equations and 0.001 pu for voltage equations. Table I only shows the mismatches above these tolerances, with the corresponding equations (some of them are found in Appendix A).

TABLE I

CASE 1. FINAL MISMATCHES AT THE SINGULARITY POINT

eqn. group	eqn. type	system component	final mismatch
(4)	active current	bus 1042	-0.7 MW/pu
(5)	(16)	generator g6	0.7 MW

Clearly the method points out generator g6 as being responsible for the singularity, with a mismatch on the active power balance equation of this generator and the active current balance equation of the bus where it is connected.

To check the validity of this diagnosis a time simulation was run with the detailed model (1-3) from which the QSS model was derived.

The corresponding voltage evolutions are shown in Fig. 3. As can be seen, over the time interval of the QSS simulation, both models yield very similar voltage evolutions (except of course the stable electromechanical oscillation neglected in the QSS model). The detailed simulation, however, shows a final collapse that corresponds to instability of the short-term dynamics. This is confirmed by the rotor angle curves of Fig. 4, relative to generators in the central area (all angles

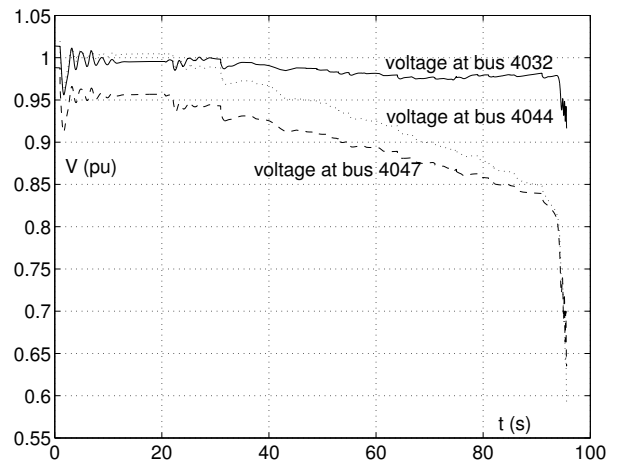


Fig. 3. Case 1. Time evolution of voltages - detailed simulation

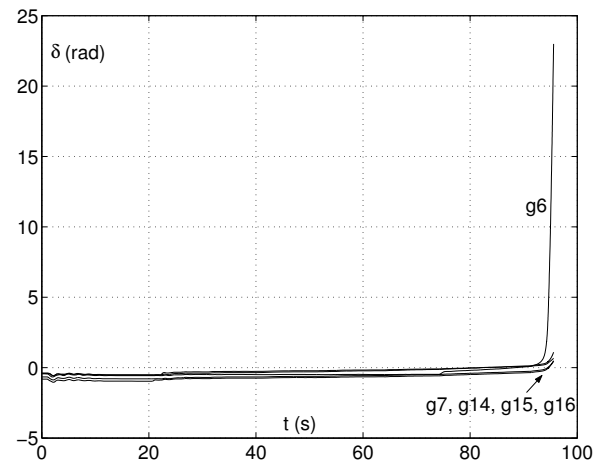


Fig. 4. Case 1. Time evolution of rotor angles - detailed simulation

are referred to that of generator g20). The curves clearly show that generator g6 is going out step, dragging some other nearby generators. This nicely corroborates the results of Table I.

This angular instability corresponds to a loss of equilibrium of the system, caused by a lack of synchronizing torque on the field current limited generator g6 [2]. Under the effect of constant excitation and sagging network voltages, the maximum electromagnetic torque of that generator decreases progressively until it becomes smaller than the mechanical torque imposed by its turbine, making steady-state synchronous operation impossible.

We note that QSS singularity occurs at  $t = 79$  s while synchronism is lost near  $t = 95$  s. This is explained by (i) the QSS assumption that short-term dynamics are infinitely fast, which stops being true (see Section II.B); (ii) the time taken by the loss of equilibrium to reveal, owing to rotor inertia.

### C. Case 2

The same disturbance is simulated but a longer thermal overload capability is assumed for g6, allowing this machine to be overexcited over the whole simulation.

A singularity is met in the QSS simulation at  $t = 86$  s,

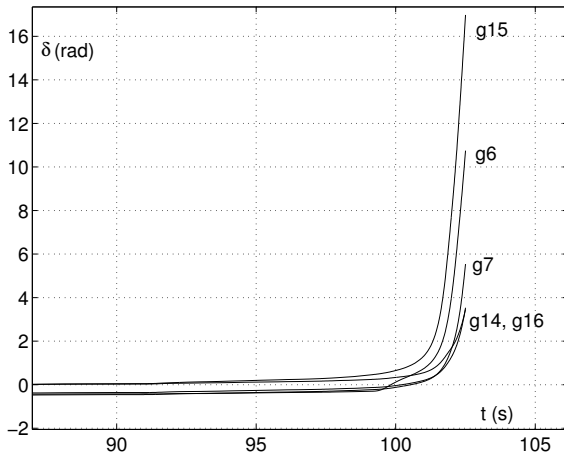


Fig. 5. Case 2. Final evolution of rotor angles - detailed simulation

following two LTC step changes. The final significant mismatches are given in Table II. They point out generator g15.

TABLE II  
CASE 2. FINAL MISMATCHES AT THE SINGULARITY POINT

eqn. group	eqn. type	system component	final mismatch
(4)	active current	bus g15	0.5 MW/pu
(4)	reactive current	bus g15	-0.6 Mvar/pu
(4)	active current	bus 4043	-0.7 MW/pu
(4)	active current	bus 4047	-1.0 MW/pu
(5)	(16)	generator g15	-1.7 MW

As in the previous case, the detailed simulation ends up in a loss of synchronism. The final rotor angle evolution is shown in Fig. 5. Generator g15 is indeed the first to go out of step.

It must be noted, however, that g15 is accompanied by other machines, which are not pointed out by the mismatches of the optimal multiplier technique. Indeed, the latter tends to concentrate the mismatches on few equations. Furthermore, it does not take into account the influence of rotor inertia. Hence, when the angular instability mode involves several generators, the proposed method might fail to identify all of them. Nevertheless, in a large system, it will successfully point out the area of concern.

#### D. Case 3

In this case, the field current limit of generator g14 is set to a conservatively low value. As a result, this machine loses synchronism shortly after its OEL is activated, at  $t = 22$  s, under the effect of the initial disturbance. This instability of the short-term dynamics occurs before any long-term effects of LTCs and other OELs.

In the QSS simulation, a singularity is met right when attempting to enforce the field current limit. The system QSS evolution is reduced to the first 22 seconds of that found in the first case.

Tables III and IV show the largest final mismatches when  $E_q$  (the emf proportional to field current; see Appendix A) is limited to 2.3 and 2.2 pu, respectively, instead of the correct 2.80 pu value.

TABLE III  
CASE 3. LARGEST FINAL MISMATCHES;  $E_q$  LIMITED TO 2.3 PU

eqn. group	eqn. type	system component	final mismatch
(4)	active current	bus g14	-14.9 MW/pu
(4)	reactive current	bus g14	-8.1 Mvar/pu
(4)	active current	bus g15	-0.6 MW/pu
(4)	active current	bus 4042	-4.1 MW/pu
(5)	(16)	generator g14	-19.5 MW
(5)	(16)	generator g15	-0.7 MW

TABLE IV  
CASE 3. LARGEST FINAL MISMATCHES;  $E_q$  LIMITED TO 2.2 PU

eqn. group	eqn. type	system component	final mismatch
(4)	active current	bus g14	-31.4 MW/pu
(4)	reactive current	bus g14	-25.1 Mvar/pu
(4)	active current	bus g15	-1.8 MW/pu
(4)	reactive current	bus g15	0.6 Mvar/pu
(4)	reactive current	bus 4011	-0.8 Mvar/pu
(4)	active current	bus 4021	-0.9 MW/pu
(4)	reactive current	bus 4021	-0.7 Mvar/pu
(4)	reactive current	bus 4022	-0.7 Mvar/pu
(4)	active current	bus 4031	-0.7 MW/pu
(4)	active current	bus 4032	-0.7 MW/pu
(4)	active current	bus 4042	-7.5 MW/pu
(4)	active current	bus 4043	-1.0 Mvar/pu
(4)	active current	bus 4044	-0.7 Mvar/pu
(5)	(16)	generator g14	-44.0 MW
(5)	(16)	generator g15	-2.0 MW
(5)	(16)	generator g16	-0.6 MW

Both tables show significantly larger mismatches than in Cases 1 and 2, indicating a more severe loss of equilibrium. As a result, non negligible mismatches are left on other generators than g14 and other buses than 4047. Nevertheless, the largest values point out g14 unambiguously as the cause of the singularity. As can be expected, the lower the limited current, the larger the mismatch relative to Eq. (16), denoting a larger gap between mechanical and electromagnetic torques.

#### E. Numerical aspects

Finally, we show the numerical performance of the optimal multiplier technique. All results refer to Case 1.

The QSS simulation uses a time step size of 1 second and relies on the “dishonest” Newton scheme, in which the Jacobian matrix  $\varphi_u$  is updated as few as possible. At each time step, the iterations are initialized with the state vector of the previous step. Over the 79 seconds of the QSS simulation, Newton iterations are performed at 28 time steps with an average of 2.3 iterations per step. The Jacobian is updated only 10 times, when the disturbance is applied and when machines are switched under field current limit.

At  $t = 79$  s, when the singularity is met, the standard Newton scheme is stopped after 7 iterations, when the  $\rho$  function is found to increase.  $u$  is then reset to its initial value, and the optimal multiplier method is applied, with the Jacobian updated at each iteration. The iterations are shown in Table V. Three iterations are performed, before  $\lambda_{min}$  reaches zero, indicating that the equations cannot be solved. The variation of  $\rho$  with  $\lambda$  at the second iteration is shown in Fig. 6, where the numbers indicate the sequence of tested points.

In the line search, the tolerance on  $\lambda$  is set to 0.025; with



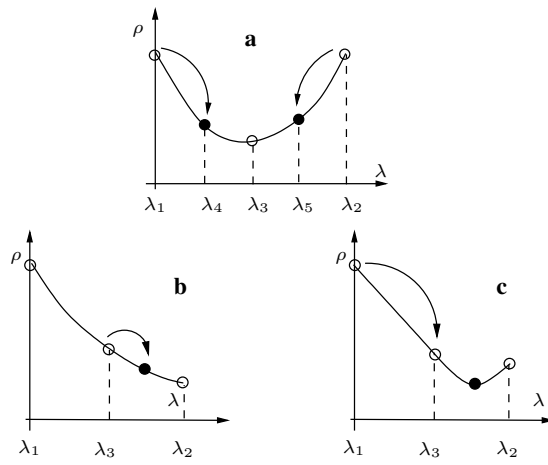


Fig. 7. Subdividing the search interval

#### APPENDIX B. LINE SEARCH PROCEDURE

The procedure is analog to a binary search for finding function roots. It starts with the evaluation of the function to be minimized at three consecutive points  $\lambda_1, \lambda_3, \lambda_2$ . It then consists of building smaller and smaller intervals  $[\lambda_1, \lambda_3, \lambda_2]$  in which we are guaranteed to find the minimum.

The procedure starts with  $[\lambda_1, \lambda_2] = [0, 1]$ . A new value  $\lambda_3$  is taken in the middle of the interval and  $\rho(\lambda_3)$  is computed.

Consider first the situation depicted in Fig. 7.a, where:

$$\rho(\lambda_3) < \rho(\lambda_1) \text{ and } \rho(\lambda_3) < \rho(\lambda_2). \quad (24)$$

We only know that the function has its minimum somewhere between  $\lambda_1$  and  $\lambda_2$ . To further “bracket” the minimum,  $\rho$  is computed at two other points  $\lambda_4$  and  $\lambda_5$ . The new smaller interval including the minimum is formed by three consecutive values of  $\lambda$ , the middle one corresponding to the smallest value of  $\rho$  computed so far. In other words, the new  $\lambda_3$  is the element of  $\{\lambda_3, \lambda_4, \lambda_5\}$  yielding the smallest  $\rho$  value. In the example of Fig. 7.a,  $\lambda_3$  does not change and the new interval is  $[\lambda_4, \lambda_3, \lambda_5]$ .

Note that two function evaluations, as in Fig. 7.a, are not necessarily needed. Indeed, if the first point considered, say  $\lambda_4$ , brings a lower function value than the central point, i.e.  $\rho(\lambda_4) < \rho(\lambda_3)$ , it is useless to try a second point, since both new points could not be lower than the central point under the assumption of a single minimum in the search interval.

Consider now the situation depicted in Figs. 7.b and 7.c, where the three points do not satisfy (24), but rather make up a decreasing sequence. Clearly, either the minimum is  $\lambda = 1$ ,

as in Fig. 7.b, or is somewhere in the interval  $[\lambda_3, \lambda_2]$ , as in Fig. 7.c. When partitioning this interval, either a new decreasing sequence is found, as in Fig. 7.b, or the values satisfy (24), as in Fig. 7.c, in which case we are brought back to the situation of Figs. 7.a. Increasing sequences are obviously handled in the same way, with possible convergence towards  $\lambda = 0$ .

The above procedure is repeated until the difference between the upper and lower bounds of the interval is smaller than a specified tolerance. In all cases, we place a new point in the middle of the surrounding interval.

This technique is a variant of the golden section search, which considers unequal partitioning of the search interval. With respect to the latter, the above described approach guarantees that the interval is divided by two at each iteration, possibly at the price of a few additional function evaluations.

#### REFERENCES

- [1] P. Kundur, *Power System Stability and Control*, New York, Mc Graw Hill, 1994
- [2] T. Van Cutsem, C. Vournas, *Voltage Stability of Electric Power Systems*, Boston, Kluwer Academic Publishers, 1998
- [3] T. Van Cutsem, R. Mailhot, “Validation of a fast voltage stability analysis method on the Hydro-Québec system”, IEEE Trans. on Power Systems, vol. 12, pp. 282-292, 1997
- [4] S. Iwamoto, Y. Tamura, “A load flow calculation method for ill-conditioned power systems”, IEEE Trans. on Power Apparatus and Systems, vol. 100, 1981, pp. 1736-1743
- [5] N.D. Reppen, R.R. Austria, J.A. Uhrin, M.C. Patel, A. Galatic, “Performance of methods for ranking and evaluation of voltage collapse contingencies applied to a large-scale network”, Proc. Power Tech conf., Athens (Greece), Sept. 1993, pp. 337-343
- [6] T.J. Overbye, “A power flow solvability measure for unsolvable cases”, IEEE Trans. on Power Systems, vol. 9, 1994, pp. 1359-1365
- [7] T.J. Overbye, “Computation of a practical method to restore power flow solvability”, IEEE Trans. on Power Systems, vol. 10, 1995, pp. 280-287
- [8] Y. Makarov, A. Kontorovic, D. Hill, I. Hiskens, “Solution characteristics of quadratic power flow problems”, Proc. 12th Power System Computation Conference, Dresden (Germany), Aug. 1996, pp. 460-467
- [9] C.W. Taylor, *Power System Voltage Stability*, McGraw Hill, EPRI Power System Engineering series, 1994
- [10] M.-E. Grenier, D. Lefebvre, T. Van Cutsem, “Quasi steady-state models for long-term voltage and frequency dynamics simulation”, Proc. of the IEEE Power Tech conf., St Petersburg (Russia), June 2005
- [11] T. Van Cutsem, M.-E. Grenier, D. Lefebvre, “Combined detailed and quasi steady-state time simulations for large-disturbance analysis”, Proc. 15th Power System Computation Conference, Liège (Belgium), Aug. 2005
- [12] T. Van Cutsem, C.D. Vournas, “Voltage stability analysis in transient and mid-term time scales”, IEEE Trans. on Power Systems, vol. 11, 1996, pp. 146-154
- [13] W.H. Press, S.A. Teukolsky, W.T. Vetterling, B.P. Flannery, *Numerical recipes in Fortran* (2nd edition), Cambridge University Press, 1994
- [14] CIGRE TF 38.02.08 (M. Stubbe, convenor), “Long-term dynamics - Phase II”, Final report, January 1995